Advanced Sensor Deployment for Distribution System State Estimation and Fault Identification

Priti Paudyal[a], Kumar Utkarsh[a], Santosh Veda[a], Amir Cohen[b], Eyal Miron[b]
[a]*National Renewable Energy Laboratory, Golden, CO,* [b]*Electrical Grid Monitoring Ltd., Rosh Haayin, Israel*

***Abstract*—Distribution systems are currently facing steep operational challenges as a result of the rapidly increasing integration of renewables and other distributed energy resources (DERs) at both the primary and secondary circuit levels. Distribution utilities and system operators have traditionally had some visibility of their primary circuits using low-frequency supervisory control and data acquisition systems, and they have had very poor if not zero visibility of the secondary circuits where the presence of DERs is constantly increasing. Therefore, this paper presents simulation studies to demonstrate the benefits of an advanced, high-fidelity sensor technology, called as the Meta-Alert System (MAS), developed by Electrical Grid Monitoring, Ltd. (EGM), on the distribution grid. First, a reliable model of the EGM sensors is developed, and then two use cases—distribution system state estimation (DSSE) and fault identification—are simulated to evaluate the performance of the MAS technology. Simulation results on the Electric Power Research Institute J1 feeder demonstrate that the MAS can effectively participate in system-level DSSE programs and can detect and locate faults faster than traditional distribution protection schemes.**

I. Introduction

As a result of the rapidly increasing integration of renewables and other distributed energy resources (DERs) at both the primary and secondary circuit levels, distribution systems are currently facing steep operational challenges [1], such as poor network voltage regulation, peak demand management, and resilient operation. These challenges are compounded by the fact that distribution system operators typically have poor visibility of the secondary circuits and only some visibility of the primary circuits via low-frequency supervisory control and data acquisition systems. Further, unlike transmission systems which have sufficient integration of phasor measurement units for fast and reliable network awareness, distribution systems have very low—if not mostly zero integration of such sensor units because of their very large numbers of nodes [2]. In recent years, there have been some research in the field of distribution system monitoring, control and data analytics [3], [4]. However, the advanced sensors deployment for the real-time monitoring and management of the distribution systems is still in a very early stage.

Therefore, this paper presents the work done through a collaboration between the National Renewable Energy Laboratory (NREL) and Electrical Grid Monitoring, Ltd. (EGM) [5], through Shell, Inc.'s GameChanger program at NREL (GCxN) [6], to model, simulate, and analyze the benefits and improvements from EGM's Meta-Alert System (MAS) for fast distribution system state estimation (DSSE) and rapid identification and isolation of faults in electrical networks. The functions and capabilities of EGM's multi-sensor units (MSUs) and the Meta-Alert Management System (MAMS) were first modeled numerically, and the developed sensor models were then evaluated on a realistic distribution feeder (the Electric Power Research Institute (EPRI) J1 test feeder [7]) with a high penetration of solar photovoltaic (PV) systems for two use cases: DSSE and fault identification.

DSSE is the process of determining the operation states of the power distribution network where limited measurement data are available. DSSE is becoming increasingly important in distribution networks, first because of the aforementioned reasons of increasing DER penetrations in distribution systems; and also because, unlike transmission system state estimation, DSSE needs to handle challenges in observability, low x/r ratios, unbalanced operation, communication issues, etc [8]. Therefore, this paper presents a DSSE algorithm that uses line power flow and voltage measurement data from the EGM sensors and evaluates network states efficiently to validate the use of EGM sensors in providing real-time network situational awareness to the system operator. Further, the advantage of EGM sensors for fault identification is explored by generating multiple scenarios of faults (single- and multiphase) and then studying the responses of the MAS compared to traditional schemes. Traditional schemes here refer to the typical utility distribution protection schemes, where there are a few reclosers and/or circuit breakers mostly on the primary feeder network only. Additionally, there are mostly fuses on the laterals and the secondary networks. This traditional scheme is also referred as existing approach throughout this paper.

The rest of the paper is organized as follows: Section II describes the EGM's MAS, the selected distribution feeder, the DSSE and the fault identification use cases, and sensor placement on the feeder. Section III shows the result analysis from the simulation studies, and Section IV summarizes the performance evaluation of EGM's MAS.

II. Grid simulation with Meta-Alert System

A. Meta-Alert System

The MAS is a technology solution for the electric grid that offers real-time field monitoring and advanced analytics capable of generating useful information for operation, maintenance, and engineering. It comprises MSUs attached to grid lines, communication adaptor units, and a MAMS at the control center. Multivariate sensors of the system attached to the grid provide real-time field measurements, monitoring, and event alert notifications. The distributed MSUs sense electrical parameters—such as current, voltage, frequency, and power— and output measurement reports as well as alarm notifications when applicable. The MAMS analyzes the reports

and event alarms received from the distributed MSUs and detects anomalies, develops visualizations, and suggests appropriate correction measures. In addition, the MAS is capable of measuring real time environmental information such as cable and ambient temperature, leakage detection and power imbalance. Further information on the MAS is available in [5].

Sensor and MAMS Modeling: A simplified software-based model of the MAS is developed for the simulation studies in this paper. The developed sensor model has the capabilities to output measured electrical parameters, such as root-mean-square (RMS) current, RMS voltage, frequency, and power factor. Additionally, it issues electrical reports and energy meter reports for a predefined time period, and it issues alarm notifications indicating abnormal behavior. Fig. 1 presents an example visualization of how the MAMS analytics estimates the fault type and location. A fault was applied at one line on the EPRI J1 feeder [7] used in this paper, and as a result, events were issued at different sensors. The different colors represent the voltage and current events issued. Each voltage and current event constitutes multiple states of voltage and current at the location.

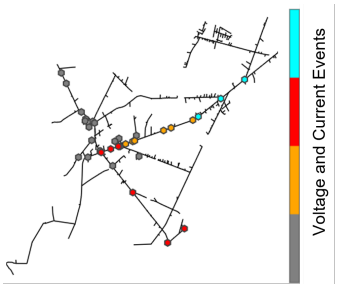

Fig. 1. Fault detection and identification visualization.

B. Use Case 1: Distribution System State Estimation

To evaluate the effectiveness of the EGM sensors in enabling DSSE using only a limited number of measurement nodes, we use the following mathematical model based on a mixed-integer weighted least square optimization:

$$\begin{aligned} \textit{minimize} \sum_{t\in T}\sum_{ij\in E}[b_{ij}\phi_{P_{ij}}^{-2}(P_{ij}^{t}-P_{ij}^{t,meas})^2 \\ + b_{ij}\phi_{Q_{ij}}^{-2}(Q_{ij}^{t}-Q_{ij}^{t,meas})^2] \\ + \sum_{t\in T}\sum_{i\in N}[b_i\phi_v^{-2}(v_i^t-v_i^{t,meas})^2] \end{aligned} \tag{1}$$

subject to:

$$P_{ij}^t = -p_j^t + \sum_{k:(j,k)\in E} P_{jk}^t + r_{ij}l_{ij}^t \tag{2}$$

$$Q_{ij}^t = -q_j^t + \sum_{k:(j,k)\in E} Q_{jk}^t + x_{ij}l_{ij}^t \tag{3}$$

$$v_j^t = v_i^t - 2(r_{ij}P_{ij}^t + x_{ij}Q_{ij}^t) + (r_{ij}^2 + x_{ij}^2)l_{ij}^t \tag{4}$$

$$l_{ij}^t v_i^t = {P_{ij}^t}^2 + {Q_{ij}^t}^2 \tag{5}$$

$$p_i^t = 0, q_i^t = 0 \text{ , if } i \in N_0 \tag{6}$$

$$\sum_{ij\in E} b_{ij} \le \hat{B} \tag{7}$$

where E is the set of lines; N is the set of nodes; P_{ij}^t and Q_{ij}^t are the active/reactive power flows in the line ij; p_i^t and q_i^t are the active/reactive power injections at node i; r_{ij} and x_{ij} are line ij's resistance and reactance; b_{ij} is a binary value denoting the presence of EGM sensors on the line ij; $\hat{B}$ is the EGM sensor budget; $P_{ij}^{t,meas}$, $Q_{ij}^{t,meas}$ and $v_i^{t,meas}$ are the values measured by the EGM sensors; T is the set of time steps at which the measurements are recorded from the EGM sensors; ϕ are the measurement variances; and N_0 is the set of nodes with no active/reactive power injections.

The minimization function (1) is a maximum likelihood estimation problem, subjected to the power flow constraints given by the DistFlow equations [9] as well as the constraints of zero-power injection at nodes known to the system operator. In the optimization model (1)-(7), the decision variables are b_{ij}, P_{ij}^t and Q_{ij}^t, while E, N, ϕ, r_{ij}, x_{ij}, and $\hat{B}$ are given parameters. Noting the non-convexity of the aforementioned problem, we employ the binary particle swarm optimization algorithm (BPSO) [10] to determine the binary values, b_{ij}, which will determine the lines at which the EGM sensors need to be present for maximum DSSE accuracy. BPSO is a discretized implementation of the continuous-space particle swarm optimization and uses the swarm intelligence concept, where a swarm of multiple solutions are iteratively evolved based on local and global function evaluations. The reader is referred to [10] for more details on the algorithm.

C. Use Case 2: Fault Identification

This use case considers a single-line-to-ground (SLG) fault, a double-line-to-ground (LLG) fault, and open-circuit fault identification. Three different analyses are considered to evaluate the fault identification use case:

- Analysis 1 : Random distribution of hundreds of faults on the feeder and calculate the percentage of faults detected.
- Analysis 2 : Apply a type of fault at a location on the feeder and evaluate the performance of each scenario with metrics. Table I provides the list of metrics considered for Analysis 2.
- Analysis 3 : Conduct Analysis 2 for all the fault scenarios in Analysis 1.

Heuristic Sensor Placement: Several factors influence the sensor placement, such as the network topology, cost of sensors, and application or use case—e.g., fault detection, state estimation, loss determination, and asset monitoring. Depending on these factors, sensors can be spread out through the network, or they can be clustered to some specific areas of interest. There are some rules/recommendations defined by EGM to place the sensors on the grid: (1) Sensors are placed on each phase, and the MAMS recognizes that relation; (2) Place the sensors before splits of the feeder for better detection resolution; or (3) Maintain the defined minimum distance between any two sensors. The best sensor location highly depends on the use case. For example, to detect more numbers of open-phase faults, sensors should be allocated toward the lateral branches in addition to major junction nodes. Fig. 2a and Fig. 2b show two sensor deployment scenarios (10% sensors) in the J1 feeder.

The performance metrics for analyses 1–3 are then compared for the following scenarios.

- S1: Traditional approach without EGM sensors

TABLE I
PERFORMANCE EVALUATION METRICS FOR ANALYSES 2 AND 3.

Performance evaluation metrics	Definition
Energy (kWh)	Total feeder energy within the simulated time frame (hours/days)
Energy lost (kWh)	Total energy not served due to fault ($Energy_{@normal} - Energy_{@fault}$)
Fault clearing time	Time consumed to restore the power back to normal condition after the crew spots the exact fault location
Total restoration time	Time from the start of the fault to normal operation
Fault location identification time	Time taken to identify the location of fault

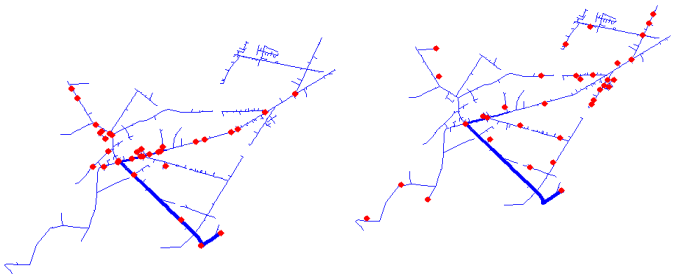

(a) (b)

Fig. 2. 10% sensor deployment Scenarios; (a) sensors are placed mostly on the major lines and at junction points, (b) sensors are placed at some end lines (lateral branches) in addition to junction points.

- S2: Heuristic placement of EGM sensors on 10% of the lines on the feeder (34 sensor units)
- S3: Heuristic placement of EGM sensors on 20% of the lines on the feeder (69 sensor units)

III. SIMULATION RESULTS AND ANALYSES

Outcomes and analyses from the simulation are presented in this section. Table II presents the threshold value fed to the sensor model to detect different event parameters.

TABLE II
THRESHOLD VALUES DEFINED TO DETECT ABNORMAL EVENTS BY THE SENSORS IN THE J1 FEEDER SIMULATION.

Parameter	Threshold
No current	Less than 2 A
No voltage	Less than than 50 V
Overcurrent	Exceeding 700 A
Overvoltage	Greater than 30% feeder nominal voltage

A. Use Case 1: Distribution System State Estimation

To analyze the effectiveness of the optimal sensor placement model presented in (1)–(7), two scenarios were simulated: 1) DSSE with random placement of EGM sensors on 10% of the lines, and 2) DSSE with optimal placement (based on (1)–(7)) of sensors on 10% of the lines. Further, each simulation was run for 1000 seconds, and line flows and node voltage measurements, i.e. $P_{ij}^{t,meas}$, $Q_{ij}^{t,meas}$ and $v_i^{t,meas}$, were recorded for each line and corresponding nodes of the system at every time-step t with 1 second granularity. Because the EGM sensors are assumed to be placed only at 10% of the lines, the accuracy of the state estimation is affected by the set of lines which actually have the sensors. This accuracy is calculated in terms of mean-squared error at each node i at a time-step t, $Error_i^t$, as follows:

$$Error_i^t = [\frac{(P_{ik}^{t*} - P_{ik}^{t,actual})^2}{\max_{t\in T, ik\in E}(P_{ik}^{t,actual})} + \frac{(Q_{ik}^{t*} - Q_{ik}^{t,actual})^2}{\max_{t\in T, ik\in E}(Q_{ik}^{t,actual})}] + [\frac{(v_i^{t*} - v_i^{t,actual})^2}{\max_{t\in T, i\in N}(v_i^{t,actual})}] \quad (8)$$

where k is a neighboring node connected to the node i, i.e. $k : (i,k) \in E$; $P_{ik}^{t,actual}$, $Q_{ik}^{t,actual}$ and $v_i^{t,actual}$ are the actual power flow and voltage values at the lines and the nodes of the system; and P_{ik}^{t*}, Q_{ik}^{t*} and v_i^{t*} are the estimated power flow and voltage values at the lines and the nodes of the system after solving the optimization model (1)-(7) by substituting the boolean variables b depending on the scenarios of random or optimal placement.

Fig. 3a and Fig. 3b show the plots for the mean-squared error $Error_i^t$ for each node, along with the average error across all the nodes, for each second of the simulation. It can be seen that for the random sensor placement scenario, the $Error_i^t$ plots have larger values when compared to those plots for the optimal sensor placement scenario. Indeed, it is observed that with random sensor placement, the average mean-square error over 1000 seconds is 0.0771%, whereas with optimal sensor placement, the average mean-square error is 0.0486%. Therefore, the optimization model presented in (1)-(7) can be used to select sensor locations for a distribution system to get maximum DSSE accuracy given a sensor budget.

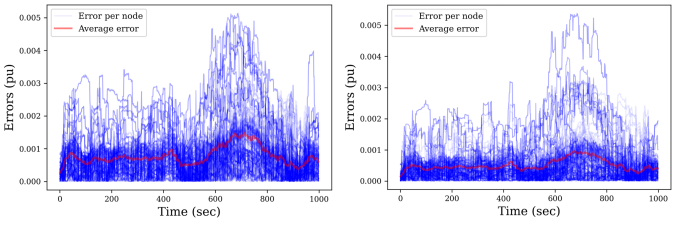

(a) (b)

Fig. 3. DSSE error plots with (a) random and (b) optimal sensor deployment on 10% of the lines.

B. Use Case 2: Fault Identification

1) Analysis 1: For Analysis 1, first, we randomly distributed 500 SLG faults one at a time on the J1 feeder, and conducted respective simulations to identify whether the fault is detected by the system. The simulation was conducted separately for all three scenarios: S1, S2, and S3 calculating the percentage of faults detected. A similar process was done considering 300 LLG faults and 300 open-phase faults. Fig. 4 shows the percentage of faults detected for all three types of faults and three scenarios. It shows that approximately 97% of the SLG faults were detected with the help of MAS, whereas the traditional approach was able to detect only 49% of those faults. Likewise, 100% of the LLG faults were detected with the MAS. On the other hand, open-phase fault detection depends on the number of sensor units placed. It requires a larger number of sensors than the two other fault types to

TABLE III
OPEN-PHASE FAULT DETECTION PERCENTAGE CHANGE WITH CHANGE IN DEPLOYMENT AND NUMBER OF SENSORS

	Scenario				
	Existing/ traditional approach	With 10% EGM		With 20% EGM	
		Deployment Scenario 1	Deployment Scenario 2	Deployment Scenario 1	Deployment Scenario 2
% of open-phase faults detected	0	34%	39%	44%	46%

detect more faults. It is evident from this analysis that the MAS deployment on the distribution feeder provides more observability of the faults than the traditional approach.

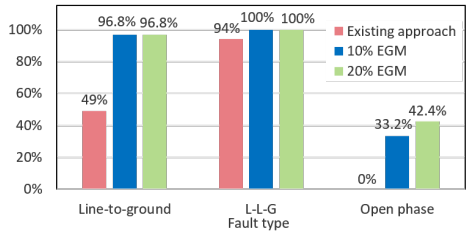

Fig. 4. Percentage of faults detected under each scenario for three different fault types.

Table III shows the change in open-phase fault detection percentage with varying placement and number of sensor units. It was observed that placing the sensors on the lateral branches in addition to some main junction points would yield a higher percentage of detection rather than allocating the sensors only to the junction points, given a limited number of sensors. Moreover, increasing the number of sensors would also increase the ability to detect more open-phase faults.

2) Analysis 2: Analysis 2 considers 1 day of simulation where a fault occurs at a location at some point of the day, and several time period assumptions are considered for the notification, identification, and clearing of the fault based on the data reported in reference [11]. Fig. 5 presents the timeline considered in this analysis for a traditional grid and the grid with MAS. The timeline in the figure represents the maximum time considering the worst-case scenario.

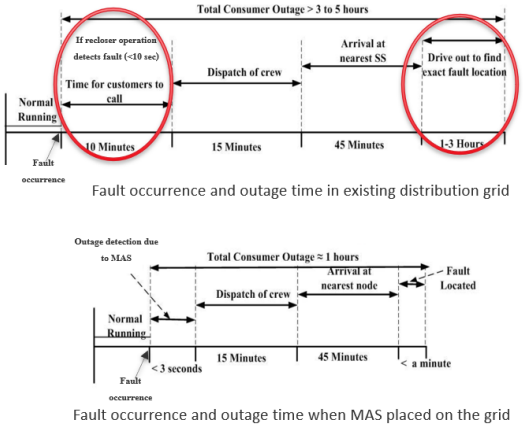

Fig. 5. Fault detection time frame for Analysis 2, reference [11]

A SLG fault was applied at the location marked in red on the lower right network plot in Fig. 6. Reclosers were placed at the green marked locations to represent the traditional grid system, where reclosers are the components that notify the fault occurrence by opening and closing the circuit in response to high fault currents.

Scenario	Performance evaluation
	Analysis 2
Baseline (normal operation)	Energy measurement (kWh) = 109,786
Fault condition (existing/traditional approach)	**Energy lost (kWh) = 24838** Fault clearing time = 45 min total restoration time = 5.75 hour Fault location identification time = 4 hour
Fault condition (10% EGM sensor placement)	**Energy lost (kWh) = 7710** Fault clearing time = 45 min total restoration time = 1.8 hour Fault location identification time = 3 min
Fault condition (10% EGM sensor placement with control)	**Energy lost (kWh) = 1476** Fault clearing time = 45 min total restoration time = 1.8 hour Fault location identification time = 3 min

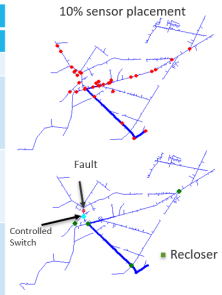

Fig. 6. Analysis 2 result metrics comparison. Fault clearing time refers to the time consumed to restore the power back to normal condition after the crew spots the exact fault location. Total restoration time is the total time from the start of the fault to the normal operating condition.

Fig. 6 shows the performance metrics calculated for Scenario 1 and Scenario 2 compared to the no-fault scenario (baseline). Clearly, having the MAS on the feeder significantly reduced the energy loss (energy not served) compared to the loss in the traditional approach. When the MAS is able to detect the fault, the location of the fault is spotted immediately, within minutes, after the repair crew reaches the estimated location. However, with the traditional approach, there could be little to no visibility into the distribution grid. So, first the crew arrive at the nearest substation and then check several points through the feeder before finding the exact fault location. That could take hours (approximately 4 hours in the given simulation condition) to pinpoint the fault. So the MAS here helps restore power much faster. Additionally, another scenario was simulated here to demonstrate the coordinated operation capability of the MAMS with the utility control system (e.g., advanced distribution management system). In this scenario, we considered that the utility has an advanced control unit that can take signals from the MAMS and sends the command to controlled switch/es to operate immediately. This could help to further reduce the energy loss from outage. Fig. 7 demonstrates the feeder total active power on the day for the considered scenarios.

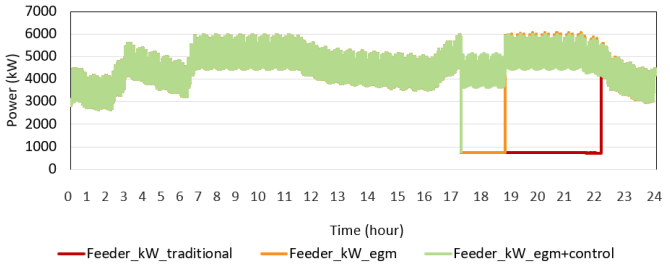

Fig. 7. Total feeder power of the day for the different scenarios considered in Analysis 2.

3) Analysis 3: Analysis 3 is the combination of both Analysis 1 and Analysis 2. A total of 300 individual SLG fault occurrences were simulated at selected random times within a day to evaluate the performance with the predefined metrics. The statistical distribution of the performance metrics—

namely, the total restoration time, total energy, and energy loss—are represented by the violin plots shown in Fig. 8 and Fig. 9. These distribution plots (violin plots) represent the 300 instances of data (corresponding to 300 different SLG faults). The wider area of a violin plot suggests that more data are concentrated around those regions, and the narrow area suggests the opposite. The total restoration time distribution in Fig. 8 shows a significant reduction in average time in the scenario with EGM compared to the traditional fault location method. The lower total restoration time with EGM implies a faster recovery from the fault events and therefore lower energy loss (energy not supplied).

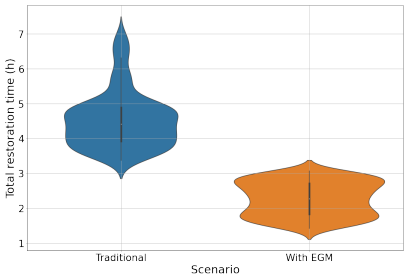

Fig. 8. Total restoration time distribution.

Comparing the distribution of the total energy supply of the traditional method to the method with the EGM sensors, the total energy supply data in the EGM method are in a higher range. The higher the total energy, the fewer customer outages. Similarly, the energy loss reduced, which means comparatively more energy was delivered, as shown in Fig. 9.

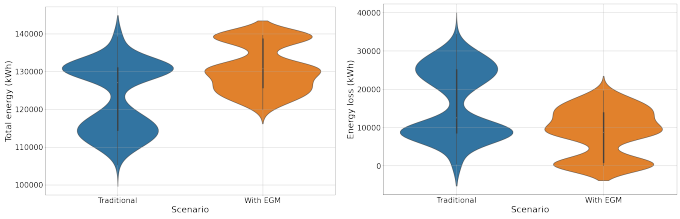

(a) (b)

Fig. 9. Total energy and loss with and without the MAS.

The comparison of the minimum, maximum, and average energy loss, Fig. 10a, and total restoration time, Fig. 10b, for the traditional method and with the EGM on the grid clarifies that the EGM system is effective at faster fault detection, identification, and restoration. This analysis implies that installing the EGM's MAS on the distribution grid could save a lot of money for utilities facing frequent fault issues.

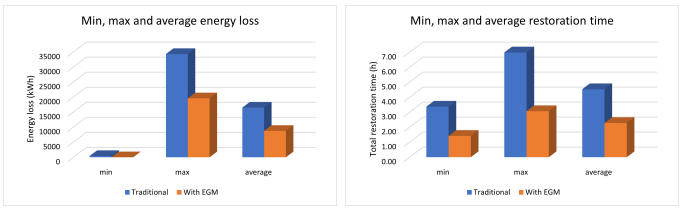

(a) (b)

Fig. 10. Minimum, maximum, and average energy loss and restoration time.

IV. Conclusion

In summary, this paper presents simulation studies to demonstrate the benefits of EGM's MAS on a distribution grid. The sensor and MAMS capabilities were first numerically modeled to investigate the DSSE and fault identification use cases. The simulation studies demonstrated that EGM's MAS can provide significantly improved DSSE accuracy with only a small number of lines with the sensors and the studies showed a significant increase in fault detection speed and accuracy, reduced down time, reduced energy lost as a result of faults, and improved customer load availability compared to traditional schemes. The EGM system was able to detect open-phase faults with good accuracy—these types of faults could not be detected by the traditional communication protection schemes modeled in the paper, and they can cause significant equipment damage if they are not cleared quickly. These improvement will help utilities provide reliable power to customers and save costs.

Acknowledgements

This work was authored in part by the National Renewable Energy Laboratory, operated by Alliance for Sustainable Energy, LLC, for the U.S. Department of Energy (DOE) under Contract No. DE-AC36-08GO28308. Funding provided through the Shell Gamechanger Accelerator Power by NREL (GCxN) program. Information is available at GCxNREL.com. The views expressed in the article do not necessarily represent the views of the DOE or the U.S. Government. The U.S. Government retains and the publisher, by accepting the article for publication, acknowledges that the U.S. Government retains a nonexclusive, paid-up, irrevocable, worldwide license to publish or reproduce the published form of this work, or allow others to do so, for U.S. Government purposes.

References

[1] C. D'Adamo, S. Jupe, and C. Abbey, "Global survey on planning and operation of active distribution networks - update of cigre c6.11 working group activities," in *CIRED 2009 - 20th International Conference and Exhibition on Electricity Distribution - Part 1*, 2009, pp. 1–4.

[2] Y. Liu, L. Wu, and J. Li, "D-pmu based applications for emerging active distribution systems: A review," *Electric Power Systems Research*, vol. 179, p. 106063, 2020. [Online]. Available: https://www.sciencedirect.com/science/article/pii/S0378779619303827

[3] M. Jamei, A. Scaglione, C. Roberts, E. Stewart, S. Peisert, C. McParland, and A. McEachern, "Anomaly detection using optimally placed microPMU sensors in distribution grids," *IEEE Transactions on Power Systems*, vol. 33, no. 4, pp. 3611–3623, 2018.

[4] M. Kezunovic, L. Xie, and S. Grijalva, "The role of big data in improving power system operation and protection," in *2013 IREP Symposium Bulk Power System Dynamics and Control - IX Optimization, Security and Control of the Emerging Power Grid*, 2013, pp. 1–9.

[5] "Solution," Jul 2019. [Online]. Available: https://egm.net/solution/

[6] Shell and NREL, "Shell gamechanger accelerator™ powered by nrel," *https://gcxnrel.com/*.

[7] E. P. R. Institute, "Epri j1 feeder," *https://dpv.epri.com/feeder_j.html*.

[8] K. Dehghanpour, Z. Wang, J. Wang, Y. Yuan, and F. Bu, "A survey on state estimation techniques and challenges in smart distribution systems," *IEEE Transactions on Smart Grid*, vol. 10, no. 2, pp. 2312–2322, 2019.

[9] M. Baran and F. Wu, "Network reconfiguration in distribution systems for loss reduction and load balancing," *IEEE Transactions on Power Delivery*, vol. 4, no. 2, pp. 1401–1407, 1989.

[10] Y. del Valle, G. K. Venayagamoorthy, S. Mohagheghi, J.-C. Hernandez, and R. G. Harley, "Particle swarm optimization: Basic concepts, variants and applications in power systems," *IEEE Transactions on Evolutionary Computation*, vol. 12, no. 2, pp. 171–195, 2008.

[11] P. Parikh, I. Voloh, and M. Mahony, "Fault location, isolation, and service restoration (flisr) technique using iec 61850 goose," in *2013 IEEE Power Energy Society General Meeting*, 2013, pp. 1–6.